



**HAL**  
open science

# Fiber-integrated optical nano-tweezer based on a bowtie-aperture nano-antenna at the apex of a SNOM tip

A. El Eter, N.M. Hameed, F.I. Baida, R. Salut, C. Filiatre, D. Nedeljkovic, E. Atie, S. Bole, Grosjean T.

► **To cite this version:**

A. El Eter, N.M. Hameed, F.I. Baida, R. Salut, C. Filiatre, et al.. Fiber-integrated optical nano-tweezer based on a bowtie-aperture nano-antenna at the apex of a SNOM tip. Optics Express, 2014, 22 (8), pp.10072-10080. 10.1364/OE.22.010072 . hal-01275266

**HAL Id: hal-01275266**

**<https://hal.science/hal-01275266>**

Submitted on 28 Dec 2023

**HAL** is a multi-disciplinary open access archive for the deposit and dissemination of scientific research documents, whether they are published or not. The documents may come from teaching and research institutions in France or abroad, or from public or private research centers.

L'archive ouverte pluridisciplinaire **HAL**, est destinée au dépôt et à la diffusion de documents scientifiques de niveau recherche, publiés ou non, émanant des établissements d'enseignement et de recherche français ou étrangers, des laboratoires publics ou privés.



Distributed under a Creative Commons Attribution 4.0 International License

# Fiber-integrated optical nano-tweezer based on a bowtie-aperture nano-antenna at the apex of a SNOM tip

Ali El Eter,<sup>1</sup> Nyha M. Hameed,<sup>1</sup> Fadi I. Baida,<sup>1</sup> Roland Salut,<sup>1</sup>  
Claudine Filiatre,<sup>2</sup> Dusan Nedeljkovic,<sup>3</sup> Elie Atie,<sup>1,4</sup> Samuel Bole,<sup>1</sup>  
and Thierry Grosjean<sup>1,\*</sup>

<sup>1</sup>*Institut FEMTO-ST, UMR CNRS 6174, Université de Franche-Comté,  
Département d'Optique P.M. Duffieux, 16 route de Gray, 25030 Besançon cedex, France*

<sup>2</sup>*Institut UTINAM, UMR CNRS 6213, Université de Franche-Comté  
Équipe Matériaux et Surfaces Structurés, 25030 Besançon cedex, France*

<sup>3</sup>*Loyalite s.a.s., 18 rue Alain Savary, 25000 Besançon, France*

<sup>4</sup>*Department of Physics, University of Balamand, Lebanon*

[\\*thierry.grosjean@univ-fcomte.fr](mailto:thierry.grosjean@univ-fcomte.fr)

**Abstract:** We propose a new concept of fiber-integrated optical nano-tweezer on the basis of a single bowtie-aperture nano-antenna (BNA) fabricated at the apex of a metal-coated SNOM tip. We demonstrate 3D optical trapping of 0.5 micrometer latex beads with input power which does not exceed 1 mW. Optical forces induced by the BNA on tip are then analyzed numerically. They are found to be  $10^3$  times larger than the optical forces of a circular aperture of the same area. Such a fiber nanostructure provides a new path for manipulating nano-objects in a compact, flexible and versatile architecture and should thus open promising perspectives in physical, chemical and biomedical domains.

© 2014 Optical Society of America

**OCIS codes:** (350.4855) Optical tweezers or optical manipulation; (130.3130) Integrated optical devices; (130.5440) Polarization-sensitive devices; (180.4243) Near-field microscopy; (250.5403) Plasmonics; (260.3910) Metal optics; (350.4238) Nanophotonics and photonic crystals.

---

## References and links

1. A. Ashkin, J. Dziedzic, J. Bjorkholm, and S. Chu, "Observation of a single-beam gradient force optical trap for dielectric particles," *Opt. Lett.* **11**(5), 288–290 (1986).
2. K. C. Neuman and S. M. Block, "Optical trapping," *Rev. Sci. Instrum.* **75**(9), 2787–2809 (2004).
3. Z. Liu, C. Guo, J. Yang, and L. Yuan, "Tapered fiber optical tweezers for microscopic particle trapping: fabrication and application," *Opt. Express* **14**(25), 510–516 (2006).
4. J.-B. Decombe, S. Huant, and J. Fick, "Single and dual fiber nano-tip optical tweezers: trapping and analysis," *Opt. Express* **21**(25), 521–531 (2013).
5. Z. Liu, L. Wang, P. Liang, Y. Zhang, J. Yang, and L. Yuan, "Mode division multiplexing technology for single-fiber optical trapping axial-position adjustment," *Opt. Lett.* **38**(14), 2617–2620 (2013).
6. H. Xin, Y. Li, L. Li, R. Xu, and B. Li, "Optofluidic manipulation of *Escherichia coli* in a microfluidic channel using an abruptly tapered optical fiber," *Appl. Phys. Lett.* **103**(3), 033703 (2013).
7. C. Liberale, P. Minzioni, F. Bragheri, F. De Angelis, E. Di Fabrizio, and I. Cristiani, "Miniaturized all-fibre probe for three-dimensional optical trapping and manipulation," *Nat. Photon.* **1**(12), 723–727 (2007).

8. S. K. Mondal, S. S. Pal, and P. Kapur, "Optical fiber nano-tip and 3D bottle beam as non-plasmonic optical tweezers," *Opt. Express* **20**(15), 180–185 (2012).
9. Y. Liu, F. Stief, and M. Yu, "Subwavelength optical trapping with a fiber-based surface plasmonic lens," *Opt. Lett.* **38**(5), 721–723 (2013).
10. M. Righini, G. Volpe, C. Girard, D. Petrov, and R. Quidant, "Surface plasmon optical tweezers: tunable optical manipulation in the femtonewton range," *Phys. Rev. Lett.* **100**(18), 186804 (2008).
11. K. Wang, E. Schonbrun, P. Steinvurzel, and K. B. Crozier, "Scannable plasmonic trapping using a gold stripe," *Nano Lett.* **10**(9), 3506–3511 (2010).
12. W. Zhang, L. Huang, C. Santschi, and O. J. Martin, "Trapping and sensing 10 nm metal nanoparticles using plasmonic dipole antennas," *Nano Lett.* **10**(3), 1006–1011 (2010).
13. Y. Tanaka and K. Sasaki, "Optical trapping through the localized surface-plasmon resonance of engineered gold nanoblock pairs," *Opt. Express* **19**(18), 462–468 (2011).
14. Y. Pang and R. Gordon, "Optical trapping of a single protein," *Nano Lett.* **12**(1), 402–406 (2011).
15. A. A. Saleh and J. A. Dionne, "Toward efficient optical trapping of sub-10-nm particles with coaxial plasmonic apertures," *Nano Lett.* **12**(11), 5581–5586 (2012).
16. M. Mivelle, I. A. Ibrahim, F. Baida, G. W. Burr, D. Nedeljkovic, D. Charrat, J.-Y. Rauch, R. Salut, and T. Grosjean, "Bowtie nano-aperture as interface between near-fields and a single-mode fiber," *Opt. Express* **18**(15), 964–974 (2010).
17. T.-P. Vo, M. Mivelle, S. Callard, A. Rahmani, F. Baida, D. Charrat, A. Belarouci, D. Nedeljkovic, C. Seassal, G. Burr, and T. Grosjean, "Near-field probing of slow Bloch modes on photonic crystals with a nanoantenna," *Opt. Express* **20**(4), 4124–4135 (2012).
18. M. Mivelle, T. S. van Zanten, L. Neumann, N. F. van Hulst, and M. F. Garcia-Parajo, "Ultrabright bowtie nanoaperture antenna probes studied by single molecule fluorescence," *Nano Lett.* **12**(11), 5972–5978 (2012).
19. R. Bachelot, C. Ecoffet, D. Deloëil, P. Royer, and D.-J. Lounnot, "Integration of micrometer-sized polymer elements at the end of optical fibers by free-radical photopolymerization," *Appl. Opt.* **40**, 5860–5871 (2001).
20. I. Ibrahim, M. Mivelle, T. Grosjean, J.-T. Allegre, G. Burr, and F. Baida, "The bowtie shaped nano-aperture: a modal study," *Opt. Lett.* **35**, 2448–2450 (2010).
21. A. Taflové and S. Hagness, *Computational Electrodynamics: The Finite-Difference Time-Domain Method*, 3rd ed. (Artech House, 2005).
22. E. X. Jin and X. Xu, "Obtaining super resolution light spot using surface plasmon assisted sharp ridge nanoaperture," *Appl. Phys. Lett.* **86**(11), 106–106 (2005).
23. C. Filiâtre, C. Pignolet, A. Foissy, M. Zembala, and P. Warszyński, "Electrodeposition of particles at nickel electrode surface in a laminar flow cell," *Colloids Surf., A* **222**(1), 55–63 (2003).
24. J. Jackson, *Classical Electrodynamics* (John Wiley, 1999).

## 1. Introduction

Since first demonstrated by Ashkin [1], optical tweezers have attracted intense research interest in the past years due to their unique ability to manipulate tiny objects without contact. Optical tweezers have been successfully used in manipulating a large panel of physical object and biological entities [2]. However, optical tweezers are often restricted, both in size of trapped particles and compactness, to being generated by diffraction limited bulky optics, and it remains a key fundamental challenge to realize optical tweezers capable of manipulating submicron particles in small, versatile and flexible configurations.

A way of addressing this issue is to make use of optical fibers which avoid the use of complex bulky optics to redirect photons. Various optical tweezers involving fiber microtips [3–6], and multicore lensed fibers [7] have been demonstrated for the 3D optical trapping of entities of a few micron size. The 3D optical trapping of submicron particles with a fiber system has recently been achieved with the development of fiber 3D bottle beams [8] and plasmonic lenses [9] which are techniques based on diffraction limited focusing.

The recent achievement of optical trapping with plasmonic nano-antennas [10–15] introduces the prospect of the manipulation of deeply subwavelength entities in a highly controlled and reproducible manner. However, the resulting optical architectures proposed so far are limited to nano-antennas fabricated on planar surfaces and excited optically with bulky optics. Recently, a single bowtie-aperture nano-antenna (BNA) has been integrated at the apex of a fiber tip and has been successfully applied as an optical nanoprobe for SNOM applications [16–18]. This

aperture type nano-antenna opened at the apex of a metal-coated tip provides a background-free and moveable optical nanosource directly excited with in-fiber illumination [16]. The signal emitted by (or collected through) the fiber tip is thus only due to the BNA resonance, there is no direct coupling between the fiber and free space optical waves. Transmission efficiency through such a fiber-integrated nano-aperture has been experimentally shown to be 150 times larger than that of a circular aperture of same opened area fabricated onto the same kind of fiber tip [17].

In this letter, we report on the 3D optical trapping of submicron particles with a BNA integrated at the apex of a fiber SNOM tip. We show here optical trapping of nano-objects still observable with a conventional microscope without fluorescence imaging techniques (preliminary step before switching to smaller particles). This study represents, to our knowledge, the first demonstration of an all-fiber optical nano-tweezer (which is not limited by diffraction). Optically-induced heating of the tip is weak enough to not affect the particle motion within the close environment of the tip. This represents promising perspectives in the optical manipulation of physical and biological entities down to the nanoscale.

## 2. BNA on fiber SNOM tip

In order to produce the fiber-integrated BNA, polymer tips (30 micrometer long, radius of curvature of 0.5 micrometer at tip apex) are first grown by photopolymerization at the cleaved end facet of a monomode (1064 nm wavelength) glass fiber [19]. The angle of the tip body is about 23°. Next, the probes are metal coated with a few nanometer thick titanium adhesion layer followed by a 150 nm thick aluminum layer to ensure robustness to optically-induced heating due to in-fiber illumination (Fig. 1(a)). Aluminum is chosen for its high conductivity at infrared frequencies leading to a strong antenna effect. Due to rotating metal coating procedure, the metal layer at the tip apex is thicker than at the flanges: we measured thicknesses of about  $220 \pm 20$  nm on sacrificial tips longitudinally cut by focused ion beam (FIB) and inspected by scanning electron microscopy (SEM). The FIB system used for this experiment is a dual beam FEI Helios 600i with a Raith Elphy Multibeam attachment. Note that the uncertainty of the metal layer thickness has no incidence onto the BNA resonance properties [20]. To avoid surface roughness at the tip apex, the metal layer is abraded over a thickness of about 70 nm by FIB from the tip side. The procedure, tested on several tips, has a good reproducibility. This results in a flat homogeneous surface at the tip apex that is a few hundreds of nanometers wide (Fig. 1(b)). Finally, a 165 nm wide BNA with square gap about 35 nm large and 45° flare angles is fabricated at the apex of the tip by FIB milling. Figures 1(c) and 1(d) display scanning electron micrographs of the resulting fiber device. The series of SEM images (a-d) is realized on the same tip.

The BNA is designed to be resonant at a wavelength of  $\lambda=1064$  nm when it is immersed in water (refraction index  $n$  of 1.315). This wavelength is located in a transparency spectral window of water. The design process is performed using three-dimensional Finite Difference Time Domain method (3D FDTD) [21] and the permittivity of the metal (aluminum) is defined with a Drude model. Figure 1(e) shows the resonance spectrum of the fiber-integrated BNA in water. The BNA is excited with an incoming gaussian beam inside the tip (see figure inset). We modeled the last 2 micrometers of the tip body before the apex. The input beam is polarized along the symmetry axis of the BNA that passes through each metal triangle's tip (called polarization axis of the BNA in the following, see the white arrow of the figure inset), and described by a single temporal pulse. The time-varying optical fields are calculated at a single grid cell at the middle of the BNA feed gap. The spectrum of the electric field is then calculated by Fourier-transforming this result and normalizing it by the spectrum calculated with the same procedure without metal (only the polymer tip is considered). We see that the BNA induces at

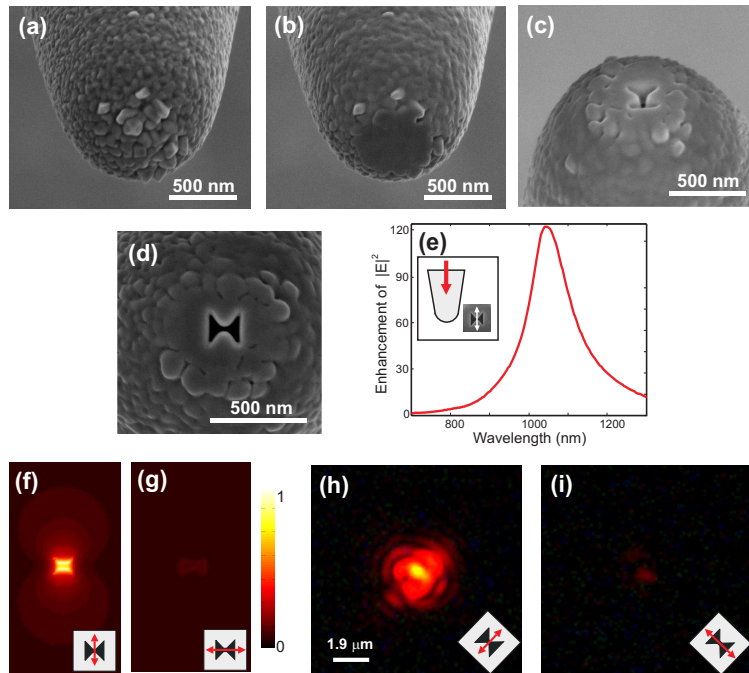


Fig. 1. (a-d) SEM micrographs of the fiber-integrated nano-tweezer based on a BNA fabricated at the apex of a SNOM tip: side view of the fiber metal-coated SNOM tip (a) before and (b) after initial FIB processing to flatten the tip apex: the rough metallic surface of the rounded apex is milled from the side to be finely polished. (c) and (d) side and top views of the BNA at the tip apex, respectively (obtained by FIB milling from the top). (e) theoretical resonance spectrum of the BNA-on-tip immersed in water: electric intensity enhancement due to the BNA. An excitation gaussian beam is injected into the 2 micrometer long end portion of the tip considered in the simulation. The optical waves are linearly polarized along the polarization axis of the BNA (see the white arrow shown in the figure inset). (f,g) Simulation of the distribution of optical electric field (amplitude) in a transverse plane (perpendicular to the tip axis) taken 10 nm away from the tip ( $\lambda=1064$  nm), for two perpendicular polarization directions of the incoming waves (see arrows in insets). (h,i) Far-field experimental images of the fiber tip output for two perpendicular polarization directions of the in-fiber illumination (BNA on and off resonance, see arrows in the insets).

$\lambda=1064$  nm a maximum 124-fold enhancement of the optical electric intensity.

Figures 1(f) and 1(g) show the simulation of the electric-field distribution (amplitude) produced by the BNA at  $\lambda=1064$  nm for an incident polarization parallel and perpendicular to the polarization axis of the nanostructure, respectively. The fields are calculated at a transverse (XY)-plane (perpendicular to the tip symmetry axis (Oz)) 10 nm away from the very tip. The electric field enhancement is induced at the BNA's feed gap by a resonant optical capacitive effect in between the two closely spaced metal triangles of the BNA, which leads to a charge distribution in the gap zone corresponding to an oscillating electric dipole [16, 22]. The dipolar properties of the BNA, which are common to all gap-based nano-antennas, associate the generation of a tiny "hot spot" to a high polarization sensitivity of the nanostructure: the tight optical confinement is canceled and the intensity maximum over the antenna is greatly reduced when the BNA is excited with optical waves polarized perpendicularly to its polarization axis (see Fig. 1(g)).

### 3. Experimental set-up

The experimental set-up developed in the frame of this study is shown in Fig. 2. The BNA on fiber SNOM tip is mounted vertically onto a manual microstage. It is immersed in a cuvette filled with a suspension of 0.5-micrometer large polystyrene latex beads (Alfa Aesar). To stay monodisperse, the particles are inserted into a cationic surfactant solution of cetyltrimethylammonium bromide (CTAB, >99% pure, Merck) at a concentration of  $5 \cdot 10^{-4}$  M [23]. The cuvette is designed to provide 0.17 millimeter-thick flat and transparent walls at two opposite sides and at the bottom for a double cross imaging procedure. The overall system is mounted onto an inverted microscope, equipped with a ( $\times 40$ , 0.5) objective, for imaging the light spot at tip apex with a CCD camera. A second (horizontal) imaging channel involving a ( $\times 60$ , 0.7) objective, a filter (to reject the laser) and a CCD camera is added to record the particle optical trapping directly with white light imaging. Note that the fiber SNOM tip is placed close to the cuvette walls to limit aberrations of the imaging systems.

The fiber is equipped with a polarization converter to define and modify the orientation of the incident polarization right at the BNA. The fiber is carefully attached on holders to prevent polarization changes during experiments. The fiber polarizer is set-up to achieve successively the two desired perpendicular polarization states right at the BNA, which lead to the maximum and minimum tip optical outputs. During this adjustment procedure, the tip emission spot is imaged with the vertical far-field imaging channel shown in Fig. 2. The two polarizer adjustments leading to the two orthogonal polarizations are recorded for the following trapping experiments.

### 4. Results and discussions

Figures 1(h) and 1(i) show far-field images of the BNA output with in fiber excitation polarized parallel and perpendicular to the BNA's polarization axis, respectively (see insets). Images are recorded during the polarization adjustment procedure detailed previously. The far-field emission of the tip achieved when the BNA is resonantly excited (Fig. 1(h)) is strongly damped when the BNA is excited off resonance (Fig. 1(i)), which is in qualitative agreement with the simulation results shown in Figs. 1(f) and 1(g). Note that the diffraction limited far-field images shown in Figs. 1(h) and 1(i) do not inform about the real spot size at the BNA.

This polarization dependent resonance property is used to demonstrate the 3D optical trapping of a submicron particle by the BNA on fiber SNOM tip (Fig. 3 and corresponding media file (Media 1)). The fiber-integrated BNA is connected with FC-PC facilities to a fiber laser diode delivering 1 mW output power. The trapping sequence shown here has a total duration of 25 seconds. From 0 to 15 seconds (see Figs. 3(a)–3(c)), the BNA is set on-resonance by orienting the incident polarization parallel to its polarization axis. From 0 to 5 seconds (see

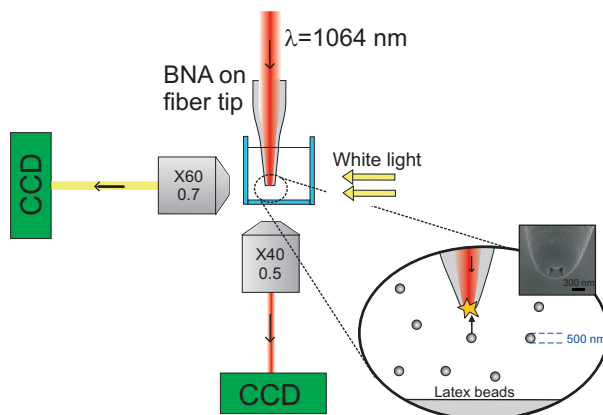


Fig. 2. Scheme of the experimental set-up.

Figs. 3(a) and 3(b)), we see that a particle close to the tip apex is pulled along vertical direction toward the tip apex (0-5s). During the last 10 seconds (Fig. 3(c)), the particle is clearly trapped at the apex of the fiber SNOM tip. Maintaining a submicron bead (3D object) at the end of a 3D conical microtip involves a 3D trapping procedure right at the tip. Then, the incident polarization is turned by  $90^\circ$  to reach non resonant regime of the BNA (Figs. 3(d)–3(f)). The initially trapped particle located at the tip apex undergoes a brownian motion of higher amplitude and leaves the tip. The trapping is no more effective. Note that the trapped bead moves here out-of-plane (it is finally hidden by the tip), which confirms that we had 3D trapping of the bead at the tip apex. The polarization sensitive trapping procedure shown here proves that the BNA is responsible for the optical phenomenon. Electrostatic forces between the particle and the tip are excluded since the particle is no more trapped when the BNA is off-resonance. The optical trapping demonstrated here is reproducible and fully governed by the BNA resonance properties: if the BNA is on-resonance, the particle stays trapped at the tip apex. Therefore, 3D trapping procedures is possible over much longer time over which the BNA is on-resonance.

The intrinsic brownian motion of the particle during trapping may a priori be reduced by enhancing the input power (a stiffer trapping is reached with higher field gradients right at the BNA). In this preliminary study, we set the input power at a level allowing unambiguous demonstration of the 3D optical trapping while ensuring preservation of our sharp polymer tip from irreversible damage due to tip heating (polymer melt). In the present experiment, no heating effect is observed onto the particle motion close to the tip. Note that increasing the input power may enhance the optical forces but it may also enhance brownian motion due to a temperature increase around the tip, which would not be in favor of a stiffer trapping. This point merits further investigations which are out of the scope of this proof-of-principle study of a new concept. Note however that convection movements of the beads have been observed close to the tip at input powers larger than 2.5 mW (at power about 3 mW, metal coated tips start to undergo irreversible damages).

Our results thus represent promising perspectives in the trapping and manipulation of tiny heat-sensitive samples like biological entities (cells, viruses, etc). The system can be implemented onto precision 3D translation stages or be static and protruding in fluidic devices. In both cases, a sharp tip would limit undesired mechanical friction effects in flowing viscous liquids, such as the modification of trajectory of moving particles close to a static tip or the displacement of surrounding particles during tip translation. Our tip seems to be a good com-

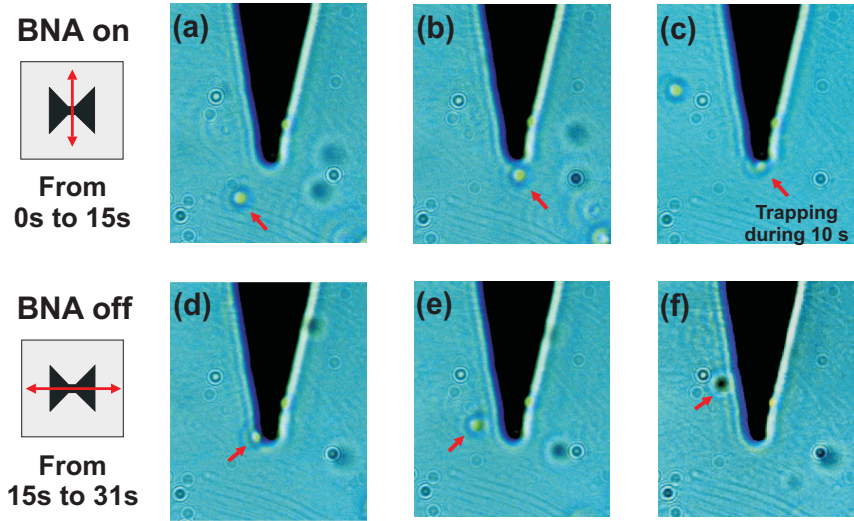


Fig. 3. Demonstration of the 3D optical trapping of a 0.5 micrometer latex bead with a BNA on fiber tip. (a-c) The polarization of the in-fiber illumination ( $\lambda=1064$  nm) is parallel to the polarization axis of the BNA: a particle is trapped at the tip apex by the BNA resonantly excited (time range from 0 to 15 seconds). (d-f) The input polarization is turned by  $90^\circ$ : the BNA is off-resonance. The initially trapped particle leaves the tip apex. The image contrast has been enhanced numerically, whereas the media file is made with raw data (see [Media 1](#)).

promise for this purpose.

## 5. Optical force analysis

The optical forces generated by the BNA on tip onto a 0.5 micrometer dielectric particle in water are analyzed numerically and compared to that of a circular aperture of the same area, on identical tip. Simulations are realized on the basis of the calculation of Maxwell's stress tensor [24] from FDTD simulations. Maxwell's stress tensor takes the following form:

$$T_{ij} = \varepsilon(E_i * E_j - \frac{1}{2} \delta_{ij} |\vec{E}|^2) + \mu(H_i * H_j - \frac{1}{2} \delta_{ij} |\vec{H}|^2), \quad (1)$$

where  $E$  and  $H$  are the electric and magnetic fields, respectively, and  $i, j$  are subscript indices corresponding to  $x, y$  or  $z$  space coordinates.  $\varepsilon$  and  $\mu$  are the dielectric permittivity and the magnetic permeability. Electric and magnetic optical fields diffracted by the dielectric particle close to the BNA are simulated with FDTD. The tip and simulation parameters are identical to that of the simulations shown previously except that now the particle ( $n=1.45$ ) is integrated within the computation volume. Note that one FDTD simulation is necessary per particle position. For each particle position, the simulated optical fields are used to calculate the Maxwell's stress tensor. Then, the optical force is deduced from the calculation of flux of the tensor through a close surface around the particle.

Figure 4(a) shows the normalized optical forces (in pN/100 mW) produced by the BNA-on-tip onto the dielectric particle aligned with respect to the tip axis ( $0z$ ). The longitudinal component of the force (along the tip axis) is plotted as a function of the distance  $d$  between the tip apex and the particle. The direction particle-toward-tip is taken positive. The transverse

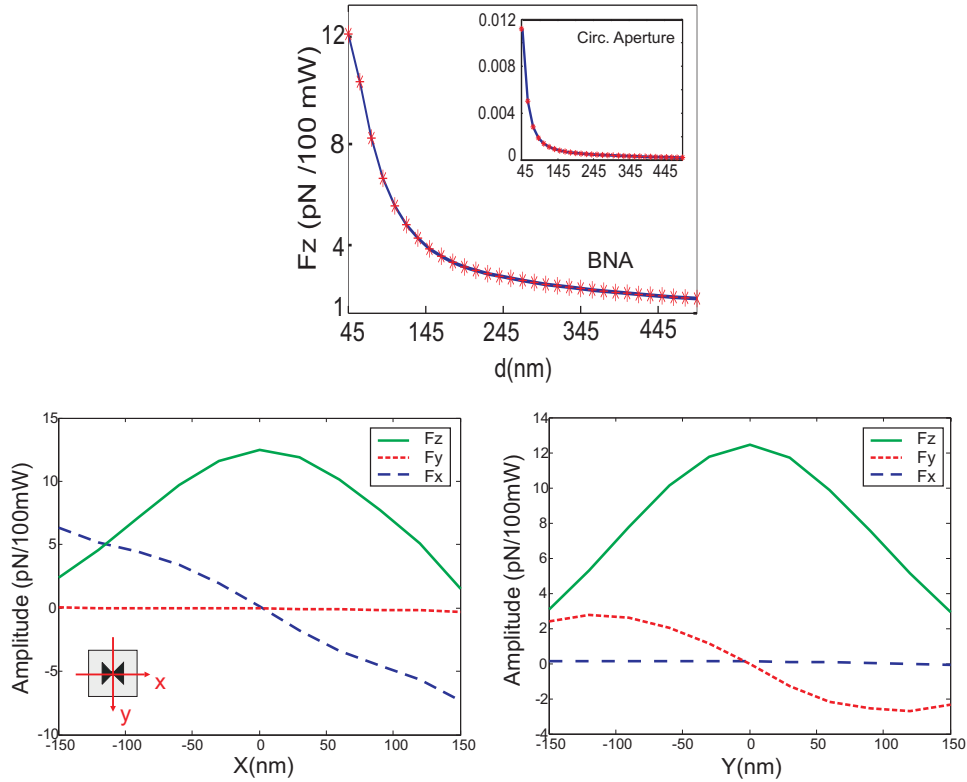


Fig. 4. Optical force induced by the BNA on tip (on resonance) onto a 0.5 micrometer dielectric nanoparticle ( $n=1.45$ ) positioned (a) along the tip axis ( $0z$ ), and (b) and (c) along the two orthogonal transverse axis ( $0x$ ) and ( $0y$ ) perpendicular to ( $0z$ ), respectively (see inset of (b) for axis orientation with respect to the BNA). (a) The longitudinal component  $F_z$  of the optical force (along the tip axis) is plotted as a function of the distance  $d$  between the BNA and the nanoparticle. The positive value of  $F_z$  means that it points toward the tip apex, which is in favor of 3D optical trapping. The transverse components of the force  $F_x$  and  $F_y$  (perpendicular to the tip axis) are negligible for these particle positions. Figure inset: longitudinal component of the optical force as a function of  $d$  for a circular aperture whose area is the same as that of the BNA (the transverse force is negligible). Forces displayed in (b) and (c) are plotted for various bead positions along ( $0x$ ) and ( $0y$ ), at a particle/tip spacing of 45 nm.  $F_z$  is still taken positive when it points toward the tip. The environment is water ( $n=1.315$ ).

components of the force  $F_x$  and  $F_y$  (perpendicular to the tip axis) are negligible for these particle positions along the tip axis. We see that the on-axis optical force points toward the BNA (since it has a positive value) and is increasing while the particle approaches the tip apex, which is consistent with an optical trapping of the particle by the BNA on tip. In the Figure inset is reported, as a function of  $d$ , the longitudinal component of the optical force produced by a circular aperture whose area is the same as that of the BNA (the transverse forces are also negligible for these particle positions). We see that the optical force shows the same behavior along the tip axis but its amplitude is  $10^3$  fold smaller. The resonance properties of the BNA induces enhanced light transmission through the tip that is linked to the generation of a tighter optical confinement, thus enhancing optical field gradients at the tip apex. Such properties are not achievable with conventional circular aperture tips which operate beyond aperture cut-off. Moreover, larger circular apertures operating under resonance would be less efficient in generating optical field gradients. This has important consequences in optical trapping down to the nanoscale. Figures 4(b) and 4(c) show the vectorial components of the optical force applied onto the bead when the bead is translated along the orthogonal transverse axis ( $0x$ ) and ( $0y$ ) perpendicular to the tip axis (see inset of Fig. 4(b) for axis orientation with respect to the BNA). It is clearly shown that the transverse components of the optical force lead to a potential well for the bead that is located at the BNA center. At this location, the longitudinal component of the force is maximum and oriented toward the tip. Therefore, the forces induced by the BNA onto the bead tend to maintain the bead at the tip apex. This is a clear numerical confirmation of the 3D trapping ability of the BNA.

## 6. Conclusion

We propose in this paper a new concept of fiber nano-tweezer based on a single bowtie-aperture nano-antenna fabricated at the apex of a fiber SNOM tip. The nano-tweezer is positioned at the end of a sharp tip instead of a bulk flat substrate, it is moveable and background-free since in-fiber illumination is used and opaque metal coated tips are considered. Our concept is demonstrated with the 3D trapping of 0.5 micron latex beads in water with 1 mW input power. The use of fiber sharp tips for tweezing limits the mechanical interaction of the tip with its environment due to liquid viscosity. We also achieve 3D optical trapping without thermal perturbation of the tip environment due to optical heating. The numerical analysis of the optical forces induced by the BNA on tip confirms the trapping ability of the nanostructure. Comparative numerical analysis of the forces produced by a BNA and a circular aperture of identical area and on identical tips reveals force amplitude  $10^3$  times higher for the BNA. Therefore, new perspectives arise in the trapping and manipulation of tiny physical and biological entities, even in media more viscous than water. Moreover, in-fiber illumination would allow the nano-tweezer to operate in turbid media. SNOM facilities for tip positioning and scanning could also be employed for tweezing.

## Acknowledgments

This work is funded by the Agence Nationale de la Recherche (ANR) under contract number ANR-10-NANO-002 ("Baltrap" project). It is supported by the "Pôle de compétitivité Microtechnique", the Labex ACTION, and the french network of technology platforms "Renatech". Tip metal coating and FIB fabrication are realized at MIMENTO technology platform.